SOLAR ENERGY COOLS MILK

O. Ayadi[1*], J. Doell[2], M. Aprile[1], M. Motta[1], T. Núñez[2]

[1]Dip. Energia, Politecnico di Milano, Milan, Italy

[2]Fraunhofer Institute for Solar Energy Systems ISE, Freiburg, Germany

[*] Corresponding Author, osama.ayadi@polimi.it

Abstract

Hot weather days cause often large fresh milk defect in southern developing countries dairy farms as well as in rural areas where there is a scarcity of energy sources that could run cooling equipments. Consequently, the possibility to use solar cooling starts to be considered an attractive solution. The aim of the work presented is to develop an innovative solar thermally driven cooling concept, to be used for received fresh milk in a dairy factory in the city of Marrakech, Morocco. The work has been carried out in the framework of the EC co-funded project (i.e., MEDISCO). The system is intended for refrigeration at 5°C in hot climates, and is composed of: medium temperature collector, single effect water ammonia absorption chiller, cold storage. The peculiarity of the configuration is the high temperature difference between the chilled refrigerant temperature, about –5 °C (in consequence of using an ice storage) and the condenser temperature (ambient temperature, which could exceed 35 °C). In these conditions, the absorption chiller must be driven by a medium temperature heat source (i.e. parabolic trough collector). Moreover, the selected chiller is directly air cooled, and has the main advantage of having no water consumption, low maintenance work and no legionella problems. . TRNSYS simulations were performed to select the appropriate system configuration, size of the solar collectors' field and the storage, heat transfer fluid and control strategy. A summary of the results is given.

Keywords: solar cooling, solar refrigeration, absorption, dairy industry.

1. Introduction

The choice of a proper solar assisted refrigeration system for hot climates , has to take into account the boundary conditions of the site and the application – i.e., level of temperature. The aim of the work presented it has been to develop an innovative solar thermally driven cooling concept, to be used for received fresh milk in a dairy factory in the city of Marrakech, Morocco. The work, carried out in the framework of the EC co-funded project MEDISCO (MEDiterranean food and agro Industry applications of Solar COoling technologies), investigated through simulations the optimum system configuration, size of the solar collectors field and the storage, heat transfer fluid and control strategy. Further a description of the system concept, industrial application load profile, model employed and simulation results is given.

2. System concept

The current work focused on a technological solution selected through a methodology based on thermodynamic analysis, as suggested in [1,2]. Following the path drawn by Henning, the combination of high temperature lift, single-effect absorption chillers, and medium temperature collectors is the only choice for solar refrigeration (low temperature cold production) under the given environmental conditions (Marrakech, Morocco).

The system concepts described in this section have been newly designed for applications under the aforementioned conditions for refrigeration in the food and agro industry. Under high ambient air temperatures (e.g., higher than 35°C) in which hardly a wet cooling tower can be employed, due to high wet bulb temperatures or no availability of water, a high temperature lift system is necessary. This is even more valid if a low cold production temperature is needed e.g., in case of ice production for cold energy storage. Under those conditions only a single-effect machine can be used if driving temperatures up to approx. 200°C are available [1,2]. Therefore if the heat source is a solar system, a collector field with optical concentration will be necessary. Tracked collector systems employing optical concentration require a climate with a high fraction of direct solar radiation on the global, which is the case for the Moroccan application object of this work. These conditions correspond very much to the needs in hot, arid regions in which fresh water is costly or a scarce commodity. Further a short description of a system based on these technologies is given.

2.1   System description

The key components of the developed system are a water-ammonia chiller (produced by Robur S.p.a.), a single-axis tracking line-focusing solar collector and a PCM storage. The system simplified scheme presented in fig. 1 is planned for refrigeration load at 5°C, serving a diary industrial process in Marrakech (Morocco). The philosophy of the integration of the solar driven plant with the existent refrigeration system aimed to keep the independence as high as possible, in term of regulation, control and moreover flexibility, feasibility and reproducibility.
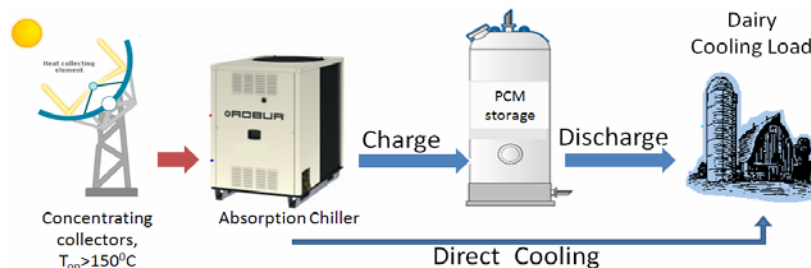
Fig. 1. Simplified scheme of the solar cooling system

3 Cooling Load Profile

In this phase of the work the aim was to create the hourly cooling load profiles of the diary Best Milk (Marrakech, Morocco). The necessary information has been provided by the factory personnel and through audits on the plant Best Milk uses raw milk provided by a vast number of farms in the area of Marrakech. Cows are milked early in the morning in small dairy farms in villages around Marrakech, then milk is collected in several collecting centres and transported by truck tanks to the diary factory in the city. Generally milk tanks reach the factory by midday and the milk temperature ranges between (9-28 °C) depending on the availability of refrigeration systems at the collecting centre and the ambient temperature. According to the process engineers, the milk has to be cooled after the first milking to 7.3°C or less within 4 h of the start of the first milking. In the existing system milk is cooled via two plate heat exchangers, supplied on their cold side with a chilled water at about 2°C. Moreover, even though with the dedicated financial resource for the project which allowed only to size the pilot system far smaller than the existing conventional one, the system design was done in a way to increase replication potential and it has been decided to work on a portion of the industrial process (i.e., a portion of the milk volume flow) which allows to speculate on the possible behaviour of the a solar refrigeration system correctly sized for the application (i.e., about seven times in capacity). A scheme of the process is given in

fig. 2. In order to investigate the opportunities of utilizing the solar cooling system in the fresh milk cooling process, both, the cooling load profile and the solar radiation for one typical summer day were studied; it was concluded that due to the mismatch between the two profiles an inertial component was needed. A cold storage has been selected to store cold energy in the phases when the availability of solar radiation allows cold production, without having concurrent cooling demand. Also, due to the existing system configuration- where there are two heat exchangers to cool milk, and they are used alternatively- it was decided to connect the solar cooled heat exchanger to play a role on cooling the return chilled water to the existing chiller as this is common between the two existing milk heat exchangers. The load profiles worked out - an example of a daily profile is presented in fig. 3 - highlighted, on a daily basis, that four operation phases take place as further described.
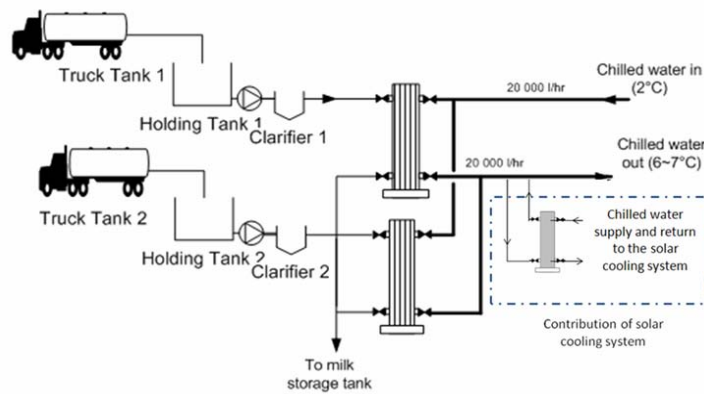
Fig. 2. Fresh milk cooling system and the integration of the solar cooling system.
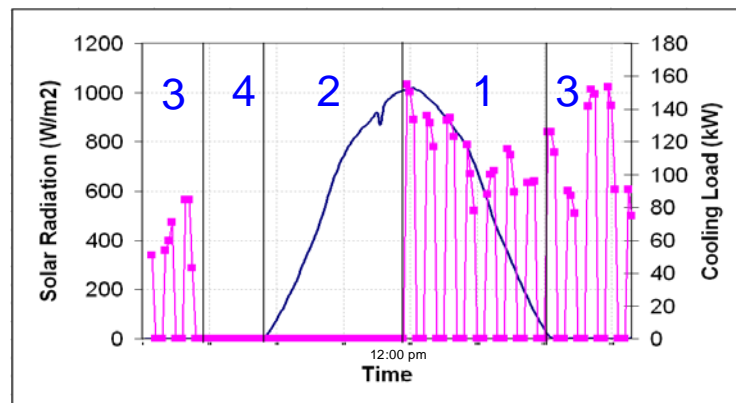
Fig. 3. Cooling load profile and the solar radiation for a typical summer day.

Operation phase:

1. Direct cooling: This is the default mode of operation of the system when there are simultaneous solar energy and cooling load.

2. Charging the cold storage: This basically happens early in the day when there is enough solar radiation to run the chiller but there is no cooling load as the milk didn't arrived yet to the factory.

3. Discharging the cold storage: As soon as the supply energy by the solar radiation is not sufficient to run the chiller, the system turns to discharge mode, where cold energy started to be discharge to the load.

4. System Off: Obviously, when there is no load and there is no solar radiation the system goes off, this mainly happens in the very late hours of the night and before sunrise.

4 System components and their models

4.1 Solar field

An essential requisite, to obtain good system efficiency, is the choice of the Solar Collector type and the working fluid, so that should be guaranteed the desired chiller operating conditions (feeding temperature, fluid flow rate etc.). As a result Roof mounted parabolic troughs RMT produced by IST and the diathermic oil were selected. In these collectors, solar energy focused and concentrated on a liquid-filled receiver dramatically reduces convection and conduction thermal

loses. The receiver/absorber is a steel tube coated with a selective blackened nickel surface and surrounded by glass. A single motor drives the collectors to track the sun continuously during the day.

4.1.1 Parabolic trough collectors modelling

To simulate the selected collectors, type 536 from the TESS library was used. This type is based on the theoretical equations developed in[3], see also[4]. This model basically follows the equation:

$$Q = R_1\, R_2\, A_{aperture}\, N_{parallel} \left[F_1\, IAM\, I_{beam} - \frac{F_2}{CR}\left(T_{in} - T_{amb}\right) \right]$$

(1)

With R_1 and R_2 as modifiers for flow correction different from the tested flow rate, $N_{parallel}$ as the number of collectors in parallel, F_1 and F_2 as the intercept and slope of the collector efficiency curve and CR as the concentration ratio of the trough. Since the collector had physically parallel rows which where connected hydraulically in series, $N_{parallel}$ was set to 1. The one-dimensional IAM-values as well as both F_1 and F_2 (0,76 and 4,17) where calculated from data provided by the manufacturer. The concentration ratio of the RMT is 7.165 (ratio of the net aperture area to the receiver area). By using an equation to reduce the incident beam radiation, the possible effect of soiling of the coated polished aluminium reflector caused by the exhaust of the nearby chimneys was taken into account. The shading of parallel rows was simulated with a shading mask (type 30) of the TRNSYS standard component library, for precise description see[5].

4.2 Absorption chiller

The absorption chiller is a derivation of Robur model ACF 60 LB, which is a single stage - gas fired - air cooled (dry fans) - aqua ammonia absorption chiller for low temperature brine generation. The chiller was adapted to cope with solar heat by replacing the gas burner with a heat exchanger wrapped around the generator. Chillers´ main technical specifications and performance figures are reported in Table1 and Figures 4 and 5 respectively.

4.2.1 Absorption chiller TRNSYS type

The absorption chiller model is a static "black box" model (see Figure6), in which experimental COP and chilling power are used to predict the chiller response at different boundary conditions. The chiller main parameters are: specific heat of oil (Cp_{oil}), specific heat of chilled water (Cp_{ch}), auxiliary power for pumps and fans operation (P_{aux}) and minimum refrigerant outlet temperature (T_{set}). The chiller inputs are: oil mass flow rate (m_{oil}), oil inlet temperature ($T_{oil,i}$), ambient temperature (T_{amb}), chilled water mass flow rate (m_{ch}), chilled water inlet temperature ($T_{ch,i}$). The

main outputs are oil outlet temperature ($T_{oil,o}$) and the chilled water outlet temperature ($T_{ch,o}$), from which driving heat rate (Q_{oil}), chilling power (Q_{ch}), rejected heat (Q_{amb}) and chiller coefficient of performance (COP) are easily calculated. For a detailed description see [7].

Table. 1. Main technical features of the Robur ACF 60 LB absorption chiller.

Parameter	Value
Nominal capacity	13 kW
Chilled water flow rate min / nom / max	2300 l/h 2500 l/h 2900 l/h
Initial charge of H_2O	11.5 kg
Initial charge of NH_3	8 kg
Max. generator pressure	35 bar
Min. evaporator temperature	-20 ^{0}C
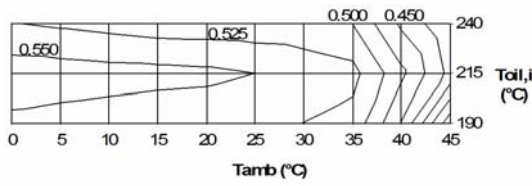
Fig. 4. COP variation with ambient temperature and oil inlet temperature for: oil flow rate 3500 l/h, chilled water inlet temperature 0 °C, chilled water flow rate 2500 l/h.
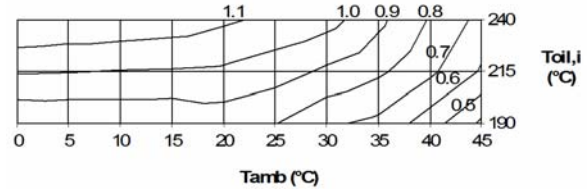
Fig. 5. Chilling power (fraction of nominal value) variation with ambient temperature and oil inlet temperature for: oil flow rate 3500 l/h, chilled water inlet temperature 0 °C, chilled water flow rate 2500l/h

Fig. 6. Absorption chiller black box model.
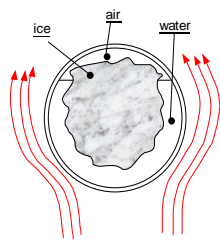
Fig. 7.. Capsule discharge phase
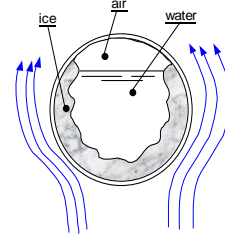
Fig8. Capsule charge phase

3. PCM storage

An ice-making storage was selected as the cold thermal energy storage system. Compared to other static ice-making systems, such as the ice-on-coil type, the ice-encapsulated type offers the advantages of low cost, simplicity and wider heat exchange area. The phase change material

(PCM), e.g., de-ionised water, is encapsulated in spherical capsules of relatively small diameter, usually in the range 50 to 100 mm. The capsules are packed into a conventional tank and the void volume around the capsules is filled with refrigerant fluid, such as water glycol solution. The phase change process is described in [6]. During charging, cool refrigerant flows around the capsules and ice starts forming from the internal surface towards the centre of the capsules (see Fig. 7.). The capsules are conceived to allow for ice expansion. During discharge, refrigerant circulates around the capsules and gets chilled by the frozen capsules. The ice starts melting, again from the internal surface towards the centre of the capsules (see Fig. 8.).

3.1 Cold storage TRNSYS type

A user-defined type was developed to describe the behaviour of an ice-making ice-encapsulated cold storage. The storage can be represented like a stack of layers (nodes), each one containing a certain number of capsules. The number of capsules in each layer is directly calculated as follows:

$$N_{capsules} = \frac{V_{tank}(1-\varepsilon)}{V_{capsule}\, N_{layers}}$$

(2)

where V_{tank} is the tank volume, $V_{capsule}$ is the capsule volume and ε is the void fraction around the capsule, typically in the range 0.4 to 0.5 depending on the capsule shape. Heat balance equations over each layer yields the following:

$$\delta_{ref} V_{ref} Cp_{ref} \frac{dT_j}{dt} = \dot{m}_{ref} Cp_{ref}\left(T_{j-1} - T_j\right) - N_{capsules} Q_{ref \to capsule} \qquad \text{when } m_{ref} \text{ is downward} \qquad (3)$$

$$\delta_{ref} V_{ref} Cp_{ref} \frac{dT_j}{dt} = \dot{m}_{ref} Cp_{ref}\left(T_{j+1} - T_j\right) - N_{capsules} Q_{ref \to capsule} \qquad \text{when } m_{ref} \text{ is upward} \qquad (4)$$

where δ_{ref}, V_{ref} and Cp_{ref} are the refrigerant density, volume and specific heat respectively, m_{ref} is the refrigerant mass flow rate, T_j is the refrigerant temperature within the j layer and $Q_{ref \to capsule}$ is the heat transferred from refrigerant to capsule. The expression for $Q_{ref \to capsule}$ depends on the particular state of the PCM inside the capsule. Four conditions are possible: 1) PCM liquid, 2) PCM in transition from liquid to solid, 3) PCM in transition from solid to liquid and 4) PCM solid. When the PCM is completely liquid or solid, the lumped capacity model is used, assuming the PCM temperature is uniform in the capsule and equal to the temperature of the layer. During PCM phase transition inside the capsule, the following experimental equations, as described in [6], have been used:

$$Q_{ref \to capsule} = 1.44 \cdot k_{ice}\left(T_j - T_{pc}\right)\cdot\left(0.12\frac{t^*}{R_o} - 1\right)^2 \quad t^* = \frac{\left(T_{pc} - T_j\right)}{L \cdot R_o^2}\frac{k_{ice}}{\delta_{ice}}t \qquad \text{when } T_j < T_{pc} \qquad (5)$$

$$Q_{ref \to capsule} = 4.00 \cdot k_{wat}\left(T_j - T_{pc}\right)\cdot\left(0.30\frac{t^*}{R_o} - 1\right)^2 \quad t^* = \frac{\left(T_j - T_{pc}\right)}{L \cdot R_o^2}\frac{k_{wat}}{\delta_{wat}}t \qquad \text{when } T_j > T_{pc} \qquad (6)$$

where L is the latent heat of water, $V_{capsule}$ is the capsule volume, R_o is the capsule radius, δ_{wat} and k_{wat} are the density and thermal conductivity of water, δ_{ice} and k_{ice} are the density and thermal conductivity of ice, T_{pc} is the phase change temperature, t is the time since phase change has started, and t^* is the dimensionless time. For a detailed description see [8].

5 Simulation results

In a parametric study, the influences of the collector field area, size of the latent heat storage (commercially available nodule ice storage), the chilled mass flow that is to be cooled and the possible effect of dust on the reflector area, were investigated. Some results are presented below.

5.1 Evaluated Parameters

To rate the system two performance figures where evaluated: The extracted heat per incident beam radiation as total efficiency (η_{total}) and the ratio between the cooling work carried out by the solar cooling system and the total cooling work required by the given process for the specified flow rate of the return flow as described in 5.3 (Solar fraction, SF).

$$\eta_{total} = \frac{Q_{extracted,solar}}{I_{beam,incident}} \quad [\%] \tag{7}$$

$$SF = \frac{Q_{extracted,solar}}{Q_{total}} \quad [\%] \tag{8}$$

5.2 Variation of collector field area and storage size

The system was simulated with different numbers of collectors and varying sizes ice storage. The parameters variation is shown in table 2.

Table 2 Simulated collector's area [m²], storage volume [m³] and capacity [kWh]

Number of collectors	11	13	15	18	20
Net aperture area [m²]	35,75	42,25	48,75	58,50	65,00

Size of storage vessel [m³]	1,5	2,0	2,5	3,0
Latent capacity [kWh]	70,4	93,9	117,4	140,8
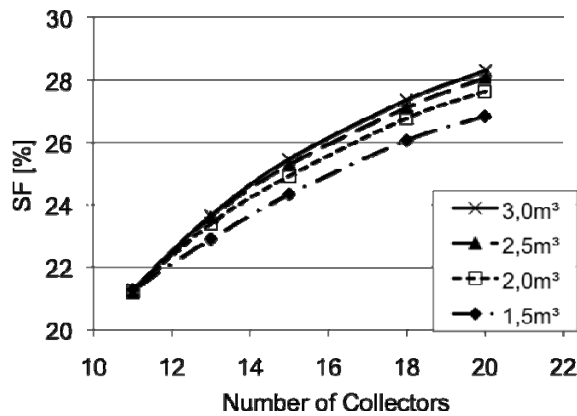
Fig. 9 Solar Fraction of the system with different storage volume
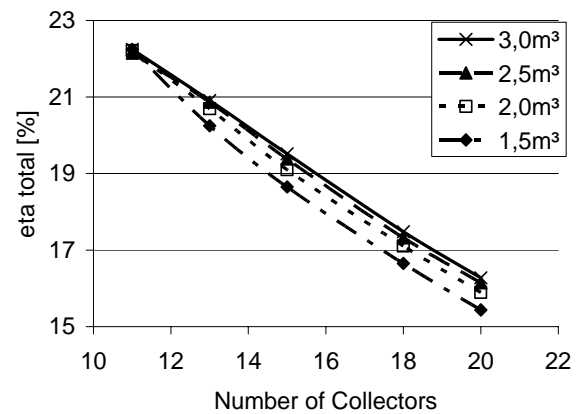
Fig. 10 Overall efficiency of the system with different storage volume

Following the results of the simulation (timestep = 1 min) are presented in the form of diagrams. The simulations highlighted that the system's solar fraction, for the given process rises with the collector field size, ranging from approximately 21 to 28% depending on the storage size. At the same time the overall efficiency of the solar system drops from about 22 to 16%. The latter is

mainly due to defocusing of the collector (dumping energy) when the solar heat input exceeds the needs (see Fig. 9). Moreover the influence of the storage size shows a milder effect on the solar fraction and system efficiency than the size of the collector field. Nevertheless it is to mention, that the influence of the storage size increases with larger collector field's areas due to the fact that part of the additional heat delivered by the bigger collector field can be stored on the "cold side" of the system. With smaller collector fields a large storage is not needed, since in most cases the smaller amount of produced cold will be extracted from the solar cooling system before the storage will be completely charged (avoiding collector defocus). Furthermore the analysis highlighted that the
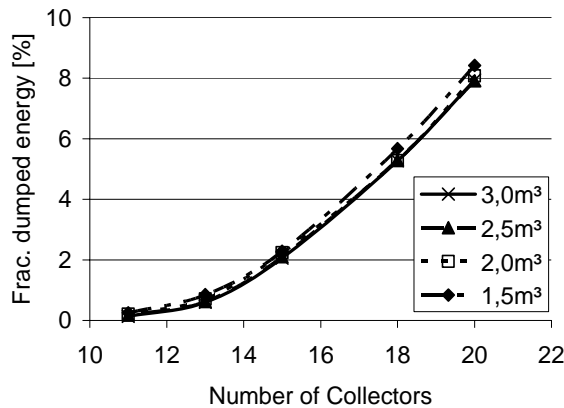
Fig. 11 Ratio of dumped energy and theoretical energy gain of the collector

maximum SF achievable (about 28%) for the system concept and application is slightly smaller than for conventional air-conditioning solar assisted systems.

5.3 Investigation of the mass flow rate in the discharging heat exchanger

Since only part of the return fluid stream of the chilled water is cooled by the solar driven absorption chiller, the influence of the system performance of the quantity of this mass flow rate was investigated. Because the mass flow on the "cold side" was more or less fixed due to the flow rate required by the absorption chiller only the "hot side" flow rate, which is the side

of the chilled water of the existing system, was changed. Three different mass flow rates were simulated: 2000, 3000 and 4000 kg/h. Results are presented, in fig. 12 and fig. 13, for the systems with 2 m³ storage volume and varying number collectors. As expected the solar fraction SF as well as the total system performance increases with higher flow rates on the "hot side" of the heat exchanger (see fig. 12).
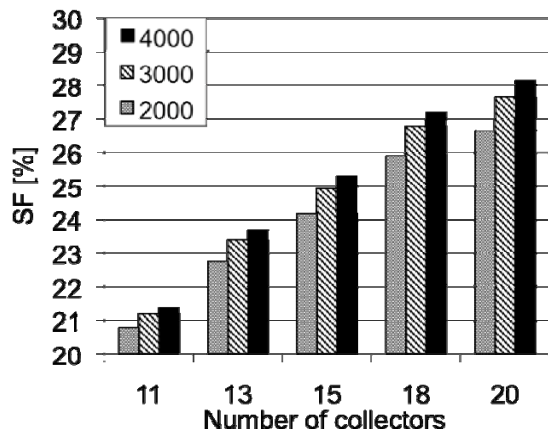
Fig. 12 Solar Fraction of the system with different mass flow rates in the HX
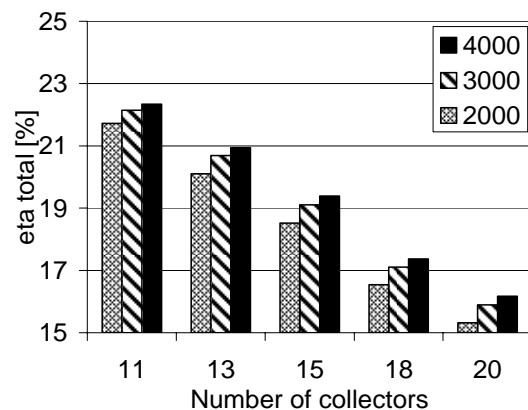
Fig. 13 Overall efficiency of the system with different mass flow rates in the HX

This is because the storage can be discharged faster (with larger temperature differences) in discharge mode. Moreover the chiller performs better in direct mode due to the higher inlet temperatures in the evaporator heat exchanger (i.e., less part load operation). Increasing the mass flow rate from 2000 kg/h to 4000 kg/h results in increment of about 1% of the solar fraction for a

specified number of collectors, However, higher flow rate means larger pump, higher costs and electricity consumption. And thus, a middle value of 3000 kg/h was selected as the flow rate for the cold side of the system.

5.4. Investigation of the effect of dust

Due to the conditions on the site some degrading of the collector reflectivity could occur due to the effect of dust exhausted by a close chimney. This effect is presented in figure 14 and figure 15 for a system with varying number of collectors, a 2 m³ storage vessel and mass flow in the HX of 3000 kg/hr.
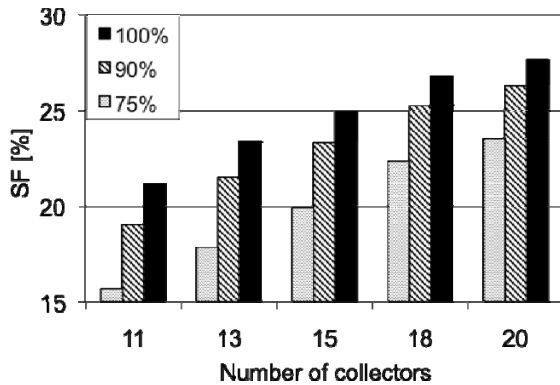
Fig. 14 Solar Fraction of the system with different fractions of cleanliness
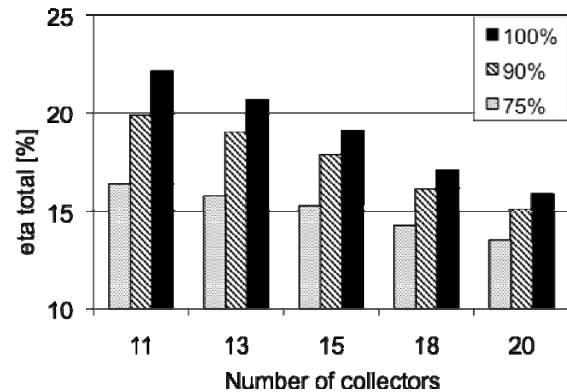
Fig. 15 Overall efficiency of the system with different fractions of cleanliness

In systems with a small collector field the effect of dust has bigger influence on the solar fraction as well as on the overall efficiency. Because a bigger amount of heat is dumped due to overheating in systems with bigger collector fields only part of the radiation lost by the effect of dust is "missing" in the system, these losses reduce the total system efficiency with about 1% .While for systems with smaller solar fields, which dump less energy are therefore more affected by the effect of dust, and these losses reduce the total system efficiency with about 5% . With respect to this effect the collector field should be designed in an appropriate way to gain the expected heat and frequent cleaning measurements should be done for the collectors to ensure high fraction of cleanliness.

6 Conclusion

The preliminary development of a solar assisted refrigeration system has been object of a simulation study with the aim to characterise the main components. The innovative concept is meant for process cooling of received fresh milk in a dairy factory in the city of Marrakech, Morocco. A portion of the process has been selected and the daily cooling load profile has been characterized: cooling power and the duration of the cooling process. The system components´ selection and system configuration was carried out to ensure the highest solar energy use considering the given cooling load profile. Moreover a parametric study on the main system components has been worked out through simulations.

Regarding the collectors' field area, its increase resulted in a growth of both, the solar fraction and the dumped energy. The latter is due to defocusing of the collectors when the input energy exceeds the demand; which can be significant for large collectors´ areas. As a result for the given

application 18 modules of parabolic through collectors were selected, in order to guarantee enough thermal energy with an acceptable amount of dumped energy.

The optimum size of the PCM storage, for the selected collector area, is 2 m^3. Considering the flow rate, a middle value of 3000 kg/h was selected as the flow rate for the cold side of the system, aiming at a compromise between increase in solar fraction and electricity costs. Three percent of the solar fraction depends on the cleanliness of the collector field, and this was taken into consideration during the sizing process as well as for the planned frequent maintenance of the system. As result of this study, the solar refrigeration system, which will be installed at the diary in Marrakech (October 2008) will consist of: 18 modules of parabolic through collectors, 2m^3 PCM storage, with cold water flow rate of 3000 kg/h.

References

[1] H. Henning, A. Häberle, A. Lodi, M. Motta; Solar cooling and refrigeration with high temperature lifts – thermodynamic background and technical solution; – Proc. of 61st National ATI Congress, ATI-IIR International Session 'Solar Heating and Cooling',14th September 2006, Perugia, Italy

[2] M. Motta, M. Aprile, H. Henning - High efficient solar assisted sorption system for air-conditioning of buildings; – Proc. of Eight international symposium gleisdorf solar, 6th – 8th September 2006, Gleisdorf, Austria.

[3] Duffie, J.A., and W.A. Beckman; Solar Engineering of Thermal Processes; J. Wiley and Sons, 1991

[4] Tess Documentation Library, chapter 10.Solar Library Technical Reference, type 536: LINEAR PARABOLIC CONCENTRATING SOLAR COLLECTOR. pp536.1-5

[5] Solar Energy Laboratory, University of Wisconsin-Madison, USA et.al.; TRNSYS 16 – a Transient System Simulation program; http://sel.me.wisc.edu/trnsys/user-resources/index.html (08.08.2008)

[6] Eams, I. W. and Adref, K. T. (2002) Freezing and melting of water in spherical enclosures of the type used in thermal (ice) storage systems. Applied Thermal Engineering. 22, pp. 733-745.

[7] M. Aprile, Simplified models implementation, MEDiterranean food and agro Industry applications of Solar COoling technologies (MEDISCO). STREP – FP6 – EU contract Project no. 032559.

[8] Aprile, M. (2006) - Simulation study of an innovative solar absorption cooling system – Master Thesis "Dalarna University" 2006.